1

Topological localization via signals of opportunity

Michael Robinson[(1)], *Member, IEEE,* Robert Ghrist[(2)]

Abstract—We consider the problems of localization, disambiguation, and mapping in a domain filled with signals-of-opportunity generated by transmitters. One or more (static or mobile) receivers utilize these signals and from them characterize the domain, localize, disambiguate, etc. The tools we develop are topological in nature, and rely on interpreting the problem as one of embedding the domain into a sufficiently high-dimensional space of signals via a signal profile function. Varying kinds of signal processing (TOA, TDOA, DOA, etc.) and discretization are addressed. Finally, we describe experiments that demonstrate the feasibility of these ideas in practice.

Index Terms—sensor networks, opportunistic signals, mapping, localization

I. INTRODUCTION

THIS article examines problems associated with localization, disambiguation, and mapping via ambient and uncontrolled signal sources of opportunity. By *localization* we mean an unambiguous, robust determination of position of receivers, transmitters, or other features of interest within an environment. We address a general setting in which the model of the environment is measureable up to *topological* features, and may lack a metric or absolute coordinate system.

We show that solving *topological* versions of localization problems is largely a matter of collecting a large enough set of signals that vary smoothly within the environment. We give precise theoretical guarantees on the number of signals required to ensure that these localization problems can be solved, as well as simulation and experimental demonstrations of its efficacy. Most other approaches aim for geometric localization, that is localization with respect to a particular background metric structure on the environment. In contrast, it should be noted that we will only require the received signals to vary smoothly as a receiver is moved within the environment, and the signals are *unconstrained* otherwise. While the received signals may arise from direct-path measurements of constant-speed waves, this restriction is strictly unnecessary. Complicated positional dependence of the signals presents no obstacle to our theory, so signals with varying speeds of propagation or multipath can be exploited as special cases.

We show how this framework also detects coarse features of the environment itself, permitting a form of topological *mapping*. We consider the case in which independent mobile sensors collect relatively coarse signal data from several transmitters, perhaps to perform inference or reconstruction

(1) Department of Mathematics, University of Pennsylvania, 209 S. 33rd Street, Philadelphia, PA 19104 USA e-mail: robim@math.upenn.edu. (2) Departments of Electrical/Systems Engineering and Mathematics, University of Pennsylvania, 209 S. 33rd Street, Philadelphia, PA 19104 USA e-mail: ghrist@seas.upenn.edu

a posteriori. We are motivated by localization in minimal-sensing scenarios with a general lack of reliable geometric information, as exemplified in (1) underground or underwater operations, (2) multistatic radar, or (3) adversarial or covert operations. (In the case of covert operations, aquiring sufficient-quality geometric data may be feasible but undesirable if it requires active sensing or excessive communication.) We begin with a continuum approximation to the problem, develop the appropriate topological tools in this setting, and then validate our assertions in simulation and experiment.

A. An elementary example

Consider an experiment with a single receiver and N transmitters with fixed, but unknown positions. The receiver is confined to lie on a compact connected line segment $\mathcal{D} \subset \mathbb{R}$, and the receivers are located in $\mathbb{R}$. The transmitters each emit a single, uniquely coded pulse that travels to the receiver, where its signal strength can be measured by a receiver when placed at any location in $\mathcal{D}$, and is stored for later reference. We do not assume synchronization of the transmitters and receiver beyond what is necessary to make this measurement, but do assume that the receiver can discriminate between different transmitters' signals. Therefore, for a given receiver location, a total of N signal strength measurements are taken (one for each transmitter). The experiment is repeated for each receiver location of interest, yielding a vector of received signal strengths for each receiver position.

Our primary question is one of *ambiguities*: does the set of signal strengths uniquely determine the position of the receiver? This question can be answered in the affirmative by considering the signal profile mapping $\mathcal{P} : \mathcal{D} \to \mathbb{R}^N$ that records the signal strength of the N (received, identified) transmitter pulses. Clearly, this map $\mathcal{P}$ is continuous, and a generic perturbation of this map embeds the interval $\mathcal{D}$ into the "signals space" $\mathbb{R}^N$ for $N > 2$. Thus, a generic choice of the signal profile mapping $\mathcal{P}$ is generically injective, implying unique channel response and the feasibility of localization in $\mathcal{D}$ via signal strength. More strongly, the continuity of such a map indicates that there is underlying robustness: nearby points in the signals space correspond to nearby points in $\mathcal{D}$.

This observation is greatly generalizable to more arbitrary domains $\mathcal{D}$, encoding both physical and temporal data. We demonstrate by theory in §**??** and experiment in §**??** that not only is the resulting signal profile map associated to signal strength injective, it also preserves topological features (holes) in the domain.

In addition, one may modify the signals space to record different aspects of signals received from the transmitters. A key insight of this paper is that replacing signal strength with

any reasonable transmitter signal space $\mathcal{S}$ and demodulation $\Phi : \mathcal{S} \to \mathcal{R}$ to a received signals space of sufficient dimension preserves the ability to localize: the injectivity of the induced SIGNAL PROFILE MAP: $\mathcal{P} : \mathcal{D} \to \mathcal{R}$ depends only on the dimension of the relevant spaces.

B. Statement of results

We assume a compact domain $\mathcal{D}$ for receivers and a *generic* (to be specified carefully) set of transmitters providing a signal profile as per the assumptions of §**??**. Under these assumptions:

1) We prove a sufficient condition for receiver localization based on opportunistic signals as a function of the number and stable coverage of transmitters. This *Signals Embedding Theorem* is independent of the signal waveform, downstream processing, and transmitter identification. This permits fusion of multiple signal types.

2) Given a discretization of the signals into geometrically small cells, we prove that preimages of these cells localize the receiver up to small cells. The diameters of these cells tend to zero as the partition of the signal domain is refined.

3) We verify our results computationally and experimentally in the context of acoutics. This demonstrates conclusively the feasibility of implementing these results in sensing contexts. Indeed, the equipment used for our experiment, though far from sufficient for the purpose of SONAR ranging or imaging, performs well for the task of detecting a change in the topology of the domain and validating our assumptions about the signal profile. Our experimental results also indicate the amount of signal corruption that such a localization system can tolerate.

We emphasize that, as the methods employed are topological, the inferences possible are likewise topological, as opposed to rigidly geometric. Changes in the topology of a domain over time (How many buildings/obstacles are present? Is the window open?) are often important.

C. Related work

There are many applications in which the signal sources are either unknown or uncontrolled, and yet their localizaton within the environment is still important. Indeed, in contrast to the problem outlined earlier, one can use a fixed network of receivers to localize a *transmitter*. One of the most direct applications of this idea is the World-Wide Lightning Localization Network [**?**], which locates lightning strikes (unknown transmitters) on the earth to within a few kilometers. This system uses a collection of radio sensors distributed on the earth's surface to correlate lightning strike arrival times. That such a distributed network can perform localization tasks under a variety of error models has been more extensively addressed in [**?**], [**?**].

Applications of opportunistic remote sensing are copious, as it is advantageous to exploit existing signal sources in the environment rather than create additional ones. Knowing a source's position, power level, and waveform can greatly

expedite its exploitation. Even in the best situation, in which the source and receiver locations are known, the required processing can be complicated [**?**]. Many of these algorithms consist of lifting traditional radar processing algorithms into a more general framework, such as Fourier transform methods [**?**], [**?**], time reversal [**?**], [**?**], equalization [**?**], [**?**], or Green's function approaches [**?**], [**?**].

Most experimental applications of opportunistic sensing in radar have focused on the use of large, publicly-recorded signal sources, such as digital broadcasters [**?**], [**?**], [**?**], [**?**], [**?**]. When such sources are not available, researchers have turned to the development of elaborate receivers with highly directive, steerable antennae [**?**]. We take a different approach, focusing on simple, inexpensive acoustic sounders that permit controlled experiments to be run in a laboratory setting.

These existing solutions suffer from a number of inherent limitations. Most evidently, they require intimate knowledge of source or receiver location and configuration. Additionally, they cannot reliably handle *multipath* (reflections, refractions, or diffractions of signals) without generating inconsistent results. Decontamination of multipath signals from a single additional scatterer was introduced in [**?**] and [**?**], with the definite understanding that this is a very limited case. More substantial multipath has the added *benefit* that if it can be correctly characterized, it can provide additional illumination for obstructed targets. When the multipath-generating scatterers are known, a filtered backprojection approach can be effective [**?**], [**?**], [**?**].

In contrast to these methods, our theory is essentially *insensitive* to multipath. Although topologically-motivated algorithms for imaging have yet to be developed, the theory described in this article provides sufficient conditions for a target's position to have a unique signal response. Questions of whether, say target paths have crossed, can be treated within our framework with relative ease. The requirements for this to succeed are simply that enough smoothly varying signal measurements can be made over the domain of interest, which is satisfied by signals in multipath settings. However, the reader is urged caution: even though a target may be localized, the resulting data may prove difficult to interpret, since embeddings of high-dimensional manifolds can be arbitrarily complicated.

Indeed, estimation of the dimension [**?**], [**?**] of the environment from this kind of signal space mapping is an interesting problem, though it appears that there is no treatment of our particular mapping in the literature. Once the dimension is known, a number of algorithms related to nonlinear compressive sensing [**?**], [**?**], [**?**], [**?**], [**?**], [**?**] could play a useful role in our analysis. In particular, they suggest that a random projection of the data to the appropriate dimension can result in an accurate *geometric* picture of the signal space. We exploit these random projections in §**??** in order to exhibit data from our experiments. However, it is worth cautioning the reader that geometric information may be irreversibly lost depending on the sensing modality. In this case, an approach like that of [**?**] permits *detection* of certain features without complete recovery of the environment.

Since projections tend to be rather limiting, one might also

suspect that manifold learning approaches, such as [?], [?], [?], [?] could provide an algorithmic basis on which to exploit the theory presented in this article. However, the performance of manifold learning algorithms tends to degrade in the presence of substantial noise (as is present in our experiment) and when there are singularities in the signal profile. Despite this, we suspect manifold learning to be a potentially valuable source of algorithms for inverting signal profiles, and active research in this area is continuing.

Our approach differs from the methods discussed previously in several important ways:

1) Our emphasis is on recovering topological features of the environment via signals of opportunity. To this end, we validate the experimental results presented in this article by computing topological invariants (persistent homology [?], [?]) of the domain as represented in the signal space and comparing them against ground truth.
2) We do not expect source or receiver locations to be known, and so focus on algorithms that are specifically non-coherent. As a benefit, algorithms developed in this framework (such as [?]) will be capable of working against poorer quality data than otherwise tolerable.
3) Our methods are robust with respect to discontinuities in received signals (near the minimum detectable signal levels) and also with respect to multipath contamination of the received signals.
4) Our framework addresses a wide array of known sensor modalities, such as those based on signal strength, time difference of arrival, direction of arrival, and more; mixed modalities are fully supported.

Finally, we address concerns about the feasibility of our approach by presenting experimental results that validate our signal model and the correctness of the resulting signal space embeddings.

II. SIGNALS AND SIGNAL PROFILES

In this section, we work in a continuum limit that permits a receiver to be located at any point in space: we will later sample this continuum by a network of fixed (or perhaps mobile) receivers in our discussion of experimental results in §**??**. All receivers reside in a compact domain $\mathcal{D}$ which is a manifold with boundary and (perhaps) corners (see Appendix for definitions from differential topology). It is common to visualize $\mathcal{D}$ as the physical workspace in which the transmitters and receivers reside, but this is not strictly necessary. For example, receivers with directional bias can be topologized as a space of cones in a tangent bundle; or, in the case where mobile receivers travel through a domain $A \subset \mathbb{R}^2$, the appropriate $\mathcal{D}$ may be the product $\mathcal{D} = A \times [0, T]$ with the time interval.

A. Spaces and signals

We give precise descriptions of the signal modalities that commonly arise in applications, though other settings can certainly be imagined. Let the environment be represented by a Riemannian manifold $\mathcal{D}$ with boundary and corners, whose global topological and geometric structure is *unknown*

to both transmitters and receivers. Represent the received signal strength from a single transmitter as the solution u to the following forced wave equation

$$c^2 \Delta u - \frac{\partial^2 u}{\partial t^2} = \delta(t - t_*, x - x_*), \ u|_{\partial D} = 0, \qquad (1)$$

where c may vary smoothly over $\mathcal{D}$. In this case, t_* and x_* represent the transmitter time and location of transmission, respectively, both of which are *unknown*.

1) **TOA:** The time of arrival (TOA) for this transmitter is defined to be the signal profile function $\mathcal{D} \to \mathbb{R}$ given by $x \mapsto \inf\{t | u(t, x) \neq 0\}$. This function is continuous and smooth except for a number of codimension-1 singularities [?], though it might not be defined on some portions of the domain. Accordingly, we assign the distinguished basepoint $\perp$ to the signal profile at such points. This makes the signal space associated to the TOA of one transmitter into the disjoint union $\mathbb{R} \sqcup \perp$. If instead of one transmitter, there are N transmitters, the resulting signals space is $(\mathbb{R} \sqcup \perp)^N$. Such a signal profile models the situation where the receiver can discriminate between signals from different transmitters, but these measurements made at the receiver may not be synchronized.
2) **TDOA:** It is often the case that the receiver has a single consistent clock. However, since the absolute timing of the transmissions is unknown, one really has the quotient of the vector of the TOA signals (one for each transmitter, as above) by the action of time translation $t \mapsto t + T$. We call this situation Time Difference of Arrival (TDOA).
3) **Strength:** Supposing the transmitted waveform to be $r = r(t)$, we define the signal strength associated with a single transmitter by the function $S(x) = \int u(s, x) r(s) ds$. If r is smooth, then the resulting signal strength is a smooth function on an open subdomain of $\mathcal{D}$.
4) **DOA:** If the receiver is equipped with a directional antenna, direction of arrival (DOA), can be extracted. Formally, it is given by the gradient of signal strength $\frac{\nabla S(x)}{\|\nabla S(x)\|}$. Observe that this can have codimension-1 singularities where the direction of arrival is undefined. Assign $\perp$ to the DOA at these points.
5) **Doppler:** Relative velocity can be measured if a single transmitter emits a pulse train while in motion, so that the source term in (**??**) takes the form $\sum_{k=0}^{M-1} \delta(t - t_k, x - x_k)$. Assuming that the pulses are far enough apart so that the receiver can discriminate between the echos associated to different pulses, and that the pulse repetition interval is known, the receiver can measure TDOA with this single transmitter. Observe that if the transmitter is moving toward the receiver, the measured differences between arrival times are decreased relative to those from a fixed transmitter.

We propose a unifying framework that considers each of the above as a special case. Consider, therefore, each transmitter to have an associated signals space $\mathcal{S}_i$. We encode limited signal

range by means of a distinguished disjoint failstate basepoint $\perp$ which connotes failure to receive or decode this signal.

B. The transmission and signal profiles

The connection between the receiver domain $\mathcal{D}$ and the spaces of signals induced by signal transmission and reception takes the form of mappings. We differentiate between the transmitted signals readable by a receiver and the information that a receiver retains after signal processing. For example, in TDOA, individual transmitter signals are detected by the receiver; however, only the time-difference between incoming signals is retained as received signal data. We encode this difference of readable and retained signals by means of a quotient map $\Phi : \mathcal{S} \to \mathcal{R}$ between the space of transmitted signals $\mathcal{S}$ and received or retained signals $\mathcal{R}$. A receiver at a point in $\mathcal{D}$ receives a transmission signal by means of a transmission profile map $\mathcal{T} : \mathcal{D} \to \mathcal{S}$ and an induced received signal profile map $\mathcal{P} : \mathcal{D} \to \mathcal{R}$, where $\mathcal{P} = \Phi \circ \mathcal{T}$.

$$\begin{array}{ccc} \mathcal{D} \xrightarrow{\;\mathcal{T}\;} \mathcal{S} = \prod_i (\mathcal{S}_i \sqcup \perp) & & \\ {}_{\mathcal{P}} \searrow \quad \downarrow {}^{\Phi} & . & \quad (2) \\ \mathcal{R} & & \end{array}$$

C. Assumptions

For the remainder of the paper, we enforce the following axiomatic characterization of signal profiles:

1) $\mathcal{D}$ is a manifold with boundary and corners.
2) The i-th transmitter emits a signal which is reliably readable by a receiver in $\mathcal{D}$ on a STABLE DOMAIN $U_i \subset \mathcal{D}$, a compact codimension-0 submanifold with corners.
3) The i-th transmitter determines a smooth TRANSMISSION MAP $\mathcal{T}_i \in C^\infty(U_i, \mathcal{S}_i)$ taking values in a TRANSMISSION SIGNAL SPACE $\mathcal{S}_i$. This space $\mathcal{S}_i$ might be 1-dimensional, as in the case of the example in §**??**. As will be detailed in examples in this article, many other choices of $\mathcal{S}_i$ are possible.
4) The i-th transmission map extends to $\mathcal{T}_i : \mathcal{D} \to \mathcal{S}_i \sqcup \perp$ and evaluates to $\perp$ on points outside of U_i.
5) The individual signal maps assemble into the TRANSMISSION PROFILE, the map $\mathcal{T} : \mathcal{D} \to \mathcal{S} = \prod_i (\mathcal{S}_i \sqcup \perp)$ given by the product of the $\mathcal{T}_i$ maps.
6) The SIGNAL PROFILE $\mathcal{P} : \mathcal{D} \to \mathcal{R}$ is the postcomposition of the transmission profile $\mathcal{P}$ with a quotient map $\Phi : \mathcal{S} \to \mathcal{R}$, where $\mathcal{R}$ is a disjoint union of manifolds and Φ is a submersion (the derivative $d\Phi$ is onto at each point of $\mathcal{S}$).

As an example, for TDOA with infinite broadcast range ($U_i = \mathcal{D}$ for $1 \le i \le N$), the quotient map Φ from the transmission signal space $\mathcal{S} = \mathbb{R}^N$ to the received time-difference space $\mathcal{R} = \mathbb{R}^{N-1}$ is a linear projection map (time-difference) with $d\Phi$ of constant rank $N - 1$ everywhere.

III. THE SIGNALS EMBEDDING THEOREM

We demonstrate that for sufficiently many generic transmission signals, each point in $\mathcal{D}$ has a unique signal profile.

The critical resource is the number (and dimension) of signals received relative to $\dim \mathcal{D}$. The collection of stable domains for the transmitters is denoted $\mathscr{U} = \{U_i\}_1^N$. It will be assumed that $\mathscr{U}$ is a cover for $\mathcal{D}$, meaning that the union of the interiors of the U_i sets contains $\mathcal{D}$. We characterize the amount of information needed to uniquely localize receivers via signals in terms of a depth of the collection of stable domains $\mathscr{U}$.

Definition 1. Given a domain $\mathcal{D}$ and a cover $\mathscr{U}$ of $\mathcal{D}$ by sets $\mathscr{U} = \{U_\alpha\}$, the DEPTH of the cover, $\mathrm{dep}\,\mathscr{U}$, is the minimal $n \in \mathbb{N}$ such that every point $x \in \mathcal{D}$ lies in at least n distinct elements of $\mathscr{U}$.

Definition 2. Consider the localization $\mathcal{T}_x : \mathcal{D}_x \to \mathcal{S}_x$ of $\mathcal{T}$ taking a neighborhood $\mathcal{D}_x$ of $x \in \mathcal{D}$ to the subspace $\mathcal{S}_x \subseteq \mathcal{S}$, which is the product of the $\mathcal{S}_i$ for which x lies in the *interior* of U_i. Define the $\mathcal{P}$-WEIGHTED DEPTH $\mathrm{dep}\,\mathcal{P}$ of the cover $\mathscr{U}$ to be the minimal rank of the derivatives $d\Phi|_{\mathcal{S}_x}$ at $\mathcal{T}_x(x)$ over all x:

$$\mathrm{dep}\,\mathcal{P} = \min_{x \in \mathcal{D}} \{\mathrm{rank}\,(d\Phi|_{\mathcal{S}_x})(\mathcal{T}_x(x))\}. \qquad (3)$$

The received signal profile $\mathcal{P}$ may or may not be injective. When it is not, receivers at different locations record identical signals. It may be the case that such ambiguity is an extreme coincidence, and a small perturbation to the individual signals removes the ambiguity in $\mathcal{P}$. On the other hand, non-uniqueness of signal profiles may be a persistent feature of the environment: although a perturbation may alter signal values at two specific receiver locations, nearby receiver locations will, after the perturbation, have identical signals. Our principal result specifies the degree of possible ambiguity.

Theorem 3 (Signals Embedding Theorem). *Let $\mathcal{P} : \mathcal{D} \to \mathcal{R}$ be a received signal profile with stable domains $\mathscr{U} = \{U_i\}_1^N$ satisfying the assumptions of §**??**. For generic transmitters — specifically, for individual transmission signal maps $\mathcal{T}_i$ open and dense in $C^\infty(U_i, \mathcal{S}_i)$ — the set of points in $\mathcal{D}$ on which $\mathcal{P}$ is non-injective is of dimension*

$$\dim\{x \in \mathcal{D} : \mathcal{P}(x) = \mathcal{P}(y) \text{ for some } y \neq x\}$$
$$\le 2\dim\mathcal{D} - \mathrm{dep}\,\mathcal{P}.$$

Proof: Begin with the following assumptions: (1) all transmissions are of unbounded extent ($U_i = \mathcal{D}$ for all i), so that $\mathcal{S} = \prod_i \mathcal{S}_i$; and (2) the quotient map Φ is the identity, so that $\mathcal{P} : \mathcal{D} \to \mathcal{R} = \mathcal{S}$. In this case, the signal profile $\mathcal{P} : \mathcal{D} \to \mathcal{R}$ is globally smooth and $\mathrm{dep}\,\mathcal{P} = \dim \mathcal{S}$. The result flows from the following version of the Whitney Embedding Theorem. A generic perturbation of the transmission signal maps $\mathcal{T}_i$ is equivalent to a generic perturbation of the received signal profile $\mathcal{P}$, since the topologies on $C^\infty(\mathcal{D}, \prod_i \mathcal{S}_i)$ and $\prod_i C^\infty(\mathcal{D}, \mathcal{S}_i)$ are equivalent [**?**]. Consider the configuration space,

$$\mathcal{C}^2 \mathcal{D} = \mathcal{D} \times \mathcal{D} - \Delta_{\mathcal{D}}$$
$$\Delta_{\mathcal{D}} = \{(x, y) \in \mathcal{D} \times \mathcal{D} : x = y\}$$

of two distinct points on $\mathcal{D}$. This is a manifold (with corners, as per $\mathcal{D}$) of dimension $2\dim\mathcal{D}$. The graph of the signal

profile $\mathcal{P}$ induces a map on the configuration space:

$$\mathcal{C}^2\mathcal{P} : \mathcal{C}^2\mathcal{D} \to \mathcal{C}^2\mathcal{D} \times \mathcal{S} \times \mathcal{S}$$
$$: (x, y) \mapsto (x, y, \mathcal{P}(x), \mathcal{P}(y)).$$

The set of points on which $\mathcal{P}$ is non-injective is precisely $(\mathcal{C}^2\mathcal{P})^{-1}(\mathcal{C}^2\mathcal{D} \times \Delta_\mathcal{S})$, where $\Delta_\mathcal{S} \subset \mathcal{S} \times \mathcal{S}$ is the diagonal. According to the multi-jet transversality theorem, cf. [**?**, Thm. 4.13], generic perturbations of $\mathcal{P}$ induce generic perturbations of $\mathcal{C}^2\mathcal{P}$ (since $\mathcal{C}^2\mathcal{P}$ is the 2-fold 0-jet of $\mathcal{P}$). Thus, from transversality and the inverse mapping theorem, the generic dimension of the non-injective set equals:

$$\dim \mathcal{C}^2\mathcal{D} + \dim \mathcal{C}^2\mathcal{D} \times \Delta_\mathcal{S} - \dim \mathcal{C}^2\mathcal{D} \times \mathcal{S} \times \mathcal{S}$$
$$= 2\dim \mathcal{D} + 2\dim \mathcal{D} + \dim \mathcal{S} - (2\dim \mathcal{D} + 2\dim \mathcal{S})$$
$$= 2\dim \mathcal{D} - \dim \mathcal{S} = 2\dim \mathcal{D} - \operatorname{dep} \mathcal{P}.$$

The transversality theorems invoked — both the multi-jet transversality and inverse mapping theorems — are usually stated for maps between smooth manifolds without boundary; however, they apply also in the case of a manifold with corners [**?**]. For a compact domain $\mathcal{D}$, as is here the case, the stronger conclusion of *open, dense* instead of *generic* holds [**?**, Prop. 5.8]. This completes the proof for the case $U_i = \mathcal{D}$ for all i and $\Phi = \mathrm{Id}$.

Next, relax the assumptions on the quotient map $\Phi : \mathcal{S} \to \mathcal{R}$ from being an identity to being a submersion — the derivative $d\Phi$ is everywhere of full rank equal to $\dim \mathcal{R} = \operatorname{dep} \mathcal{P}$. Then, following the initial case, we wish to perform perturbations in the transmission signals $C^\infty(\mathcal{D}, U_i)$, while controlling the injectivity of $\Phi \circ \mathcal{T}$. The non-injective set of $\mathcal{P}$ equals the inverse image

$$(\mathcal{C}^2\mathcal{T})^{-1} \left(\mathcal{C}^2\mathcal{D} \times (\Phi \times \Phi)^{-1}(\Delta_\mathcal{R}) \right),$$

where $\Delta_\mathcal{R} \subset \mathcal{R} \times \mathcal{R}$ is the diagonal. As Φ is a submersion, the inverse image of $\Delta_\mathcal{R}$ under the product map $\Phi \times \Phi$ is of dimension $2\dim \mathcal{S} - \dim \mathcal{R}$. Thus, from transversality and the inverse mapping theorem, the generic dimension of the non-injective set equals:

$$= 2\dim \mathcal{D} + (2\dim \mathcal{D} + 2\dim \mathcal{S} - \dim \mathcal{R})$$
$$- (2\dim \mathcal{D} + 2\dim \mathcal{S})$$
$$= 2\dim \mathcal{D} - \dim \mathcal{R} = 2\dim \mathcal{D} - \operatorname{dep} \mathcal{P}.$$

This completes the proof in the case of globally-received signals $U_i = \mathcal{D}$.

Finally, we relax to limited range signals. Assume a cover $\mathcal{U} = \{U_i\}_1^N$ of $\mathcal{D}$ of stable domains for transmission signal reception. The intersection lattice of $\mathcal{U}$ consists of all nonempty intersections of elements of $\mathcal{U}$. Let $\mathcal{V}$ denote the collection of closures of the elements of this intersection lattice. Since $\mathcal{V}$ is again a finite cover of $\mathcal{D}$ by compact codimension-0 submanifolds of $\mathcal{D}$ with corners. For convenience, use a multi-index $J \in \{\pm 1\}^N$ for $\mathcal{V} = \{V_J\}$ encoded so that

$$V_J = \operatorname{closure} \left(\bigcap_{J_i = +1} U_i \cap \bigcap_{J_k = -1} (\mathcal{D} - U_k) \right).$$

Restricting $\mathcal{T}$ to a (nonempty) V_J, yields a smooth map $\mathcal{T}_J : V_J \to \prod_{J_i = +1} \mathcal{S}_i$ (the cross product with the fail

states is ignored). By definition of the $\mathcal{P}$-weighted depth, the rank of $d\Phi$ on the image of the interior of V_J is at least $\operatorname{dep} \mathcal{P}$. Thus, as per the previous case, for an open dense set of transmission signal maps, the dimension of the non-injective set of the restriction of $\mathcal{P}$ to V_J is bounded above by $2\dim \mathcal{D} - \operatorname{dep} \mathcal{P}$. Repeating the argument for each multi-index J and taking the finite intersection of the resulting open dense sets of transmission signal maps completes the proof. ∎

IV. COROLLARIES

The Signals Embedding Theorem provides simple criteria for the signal *depth* $\operatorname{dep} \mathcal{P}$ required to ensure a generic injection into the received signals space. As is typical useage, if the dimension of the self-intersection set of $\mathcal{P}$ is negative, then $\mathcal{P}$ is understood to be one-to-one. Its image in the received signals space $\mathcal{R}$ is therefore a topologically faithful image of $\mathcal{D}$, partitioned according to $\mathcal{U}$. (This important point plays a role in our experiments, as we can detect global topological features in the image of $\mathcal{D}$ under $\mathcal{P}$.) Similarly, if the self-intersection set of $\mathcal{P}$ has dimension zero, then point ambiguities may persist in the image of $\mathcal{D}$ under $\mathcal{P}$.

A. Depth criteria for localization

In many instances, depth criteria for unique channel response is a function of the depth of the cover $\mathcal{U}$ by stable signal domains. One simply needs to consider the signal models given in §**??**.

Corollary 4. *A generic TOA or signal strength profile is injective whenever* $\operatorname{dep} \mathcal{U} > 2\dim \mathcal{D}$.

Proof: In the case of TOA or signal strength reception, each signal space $\mathcal{S}_i = \mathbb{R}$, $\Phi = \mathrm{Id}$, and $\operatorname{dep} \mathcal{P} = \operatorname{dep} \mathcal{U}$. From Theorem **??**, the subset of $\mathcal{D}$ on which $\mathcal{P}$ is generically non-injective is of negative dimension — hence empty — when $\operatorname{dep} \mathcal{U} > 2\dim \mathcal{D}$. ∎

This implies that a receiver can be localized to a unique position in a planar domain $\mathcal{D}$ using only a sequence of *five* or more locally stable TOA or strength readings from generic transmitters. For TDOA, six signals are required to achieve localization:

Corollary 5. *A generic TDOA signal profile is injective whenever* $\operatorname{dep} \mathcal{U} > 2\dim \mathcal{D} + 1$.

Proof: Each $\mathcal{S}_i = \mathbb{R}$ and the reduction map $\Phi : \mathcal{S} \to \mathcal{R}$ is a submersion of rank defect one; hence $\operatorname{dep} \mathcal{P} = \operatorname{dep} \mathcal{U} - 1$. ∎

One should contrast this result with the more familiar *triangulation* methods in use today that rely on geometric (rather than topological) data. For instance, GPS uses a TDOA method to give the precise geometric location of a receiver. Since reliable measurements can be made, only 4 satellite transmitters are required to perform the task. However, GPS suffers from multipath and ionospheric instabilities which compromise the quality of the measurements it uses. Corollary **??** indicates that not more than 8 satellites are needed

to localize the receiver even in the face of these deleterious effects.

DOA has a more dramatic effect on required signal depths.

Corollary 6. *A generic DOA signal profile is injective whenever*

$$\text{dep } \mathscr{U} > \frac{2\dim \mathcal{D}}{\dim \mathcal{D} - 1}. \tag{4}$$

Proof: Each $\mathcal{S}_i = \mathbb{S}^{\dim \mathcal{D}-1}$ and $\Phi = \text{Id}$. Thus, for injectivity,

$$2\dim \mathcal{D} < \text{dep } \mathcal{P} = (\text{dep } \mathscr{U})(\dim \mathbb{S}^{\dim \mathcal{D}-1}).$$

■

Remark 7. Note that Corollary **??** implies that
1) DOA localization is impossible when $\dim \mathcal{D} = 1$;
2) for a planar domain, there is no difference between DOA and TOA in terms of signal cover depth required; and
3) for domains of dimension greater than three, the signal depth required for DOA equals *three*, independent of dimension.

B. Time-dependent systems

1) Pulses: The simplest time-dependent system measures a pulse train, as described in item (5) in §**??**. Each pulse is audible over a stable domain U_i and induces a signal in $\mathcal{S} = (\mathcal{S}_i \sqcup \bot)^M$, where M is the number of pulses emitted and all the $\mathcal{S}_i$ are the same. Assuming that perturbation of the motion of the transmitter and the propagation of pulses induces a generic perturbation of the transmission profile map $\mathcal{T} : \mathcal{D} \to \mathcal{S}$, Theorem **??** and Corollaries **??**-**??** immediately translate to the case of a single (mobile) transmitter sending multiple pulses.

2) Path-crossing: Consider the space-time product $\mathcal{D} = \mathcal{D}' \times [0, T]$ and the case of one or more transmitters in motion in $\mathcal{D}'$. Then, in the setting of TOA, TDOA, DOA, or signal strength, one has a cover of $\mathcal{D}$ by stable patches U_i delineating where and when a signal is readable. By Theorem **??**, the signal profile map $\mathcal{P} : \mathcal{D}' \times [0, T] \to \mathcal{R}$ is injective for $\text{dep}(\mathcal{P}) > 2(\dim \mathcal{D}' + 1)$. Note well that this localizes *temporally* as well as spatially.

This injectivity criterion has additional potential utility. Assume that two mobile *receivers* move through the physical or space-time domain $\mathcal{D}$ over the time interval $[0, T]$, but have no information about their locations or relative distances. Did the receivers ever cross paths?

Note that this applies to $\mathcal{D}$ a physical or a space-time domain, allowing for determination of whether the receivers covered the same territory at *some* times or whether the receivers actually met. That such inference may be rigorously concluded *a posteriori* within the received signal space $\mathcal{R}$ seems novel. The reader may easily derive other similar generalizations for inference via received signals.

Corollary 8. *Two mobile receivers moving along paths $\gamma_1, \gamma_2 : [0, T] \to \mathcal{D}$. Their paths intersect in $\mathcal{D}$ if and only if their images in $\mathcal{R}$ under $\mathcal{P}$ intersect, assuming $\text{dep}(\mathcal{P}) > 2\dim \mathcal{D}$.*

Proof: If $\gamma_1(t) = \gamma_2(s)$ for some $t, s \in [0, T]$, the images of these points under $\mathcal{P}$ are the same. The map $\mathcal{P} : \mathcal{D} \to \mathcal{R}$ is injective since $\text{dep}(\mathcal{P})$ is large enough and the other hypotheses of Theorem **??** are satisfied; thus, if the images of γ_1 and γ_2 intersect in $\mathcal{R}$ under $\mathcal{P}$, they must have a point in common in $\mathcal{D}$. ■

C. Anonymous transmissions

The following asserts that anonymization of transmitter sources does not impact signal depth criteria.

Proposition 9. *For a signal profile in which all transmission signals are of the same type ($\mathcal{S}_i = X$ for all i) and the quotient map to $\mathcal{R}$ is equivariant with respect to transmitter identities (Φ is invariant under the action of the symmetric group S_N on $\mathcal{S}$), then passing from identified to unidentified transmitters does not change the dimension bounds on the self-intersection set in Theorem **??**.*

Proof: In our formulation, the transmission profile demands signal identities, since $\mathcal{T} : \mathcal{D} \to \prod_i(X \sqcup \bot)$. The action of the symmetric group $S_N : \mathcal{S} \to \mathcal{S}$ permuting transmitter identities descends by equivariance to an action $S_N : \mathcal{R} \to \mathcal{R}$. The quotient $\mathcal{R} \to \mathcal{R}/S_N$ is not a submersion (its derivative is not of full rank), because the action of S_N is not free[1], as in the case of two signals arriving at the same time, in which the non-identity permutation of the transmitter identities is a fixed point. However, the action of S_N *is* free (and therefore has derivative of full rank) on a *dense* codimension-0 submanifold (the complement of the Φ-image of the pairwise diagonal in X^N). The dimension bounds in the proof of Theorem **??** are sensitive only to top-dimensional phenomena; thus, $\text{dep } \mathcal{P}$ remains unchanged after quotienting by the S_N action. ■

1) Doppler: As a final (dramatic) example of dynamic transmitter-receiver localization, consider the situation of a multistatic pulsed-doppler imaging radar system in a reflective environment where there are N transmitters traveling along *unknown* paths $\gamma_k(t)$. We assume that transmitter k transmits a pulse train with an *unknown* delay t_k and a pulse repetition interval T which is *known* and common to all transmitters. The received signal is then a solution to

$$c^2 \Delta u - \frac{\partial^2 u}{\partial t^2} = \sum_{k=1}^{N} \sum_{m=0}^{M-1} U(t - t_k - mT, x - \gamma_k(t)), \; u|_{\partial D} = 0, \tag{5}$$

where U is a positive function supported within $(-T/2, T/2)$ with a unique local maximum. In order to facilitate processing, it is typical for the receiver at x to divide the received signal into blocks of length T and peak detect. Specifically, let

$$\tilde{P}(t, x) = \left\{ \tau : \frac{d}{dt}u(t - \tau, x) = 0, \text{ and} \right.$$
$$\left. \frac{d^2}{dt^2}u(t - \tau, x) < 0 \text{ for } \tau \in [0, T] \right\}.$$

Let $P(t, x)$ be the vector of length N whose components are the smallest N elements of $\tilde{P}$, padded if needed with $\bot$

---

[1]An action of a group on a set X is said to be *free* if the only group element that fixes an element of X is the identity.

if there are fewer than N elements in $\tilde{P}$. Define the signal profile to be $\mathcal{P}(t, x) = (P(t, x), \frac{dP}{dt}(t, x))$, carrying along $\perp$ as appropriate. Even in this seemingly challenging situation, the following corollary follows trivially.

Corollary 10. *A generic $\mathcal{P}$ as defined above localizes the receiver in time and space over a domain $\mathcal{D}$ whenever*

$$\kappa := \min_{t,x} \#P(t, x) > \dim \mathcal{D} + 3/2, \qquad (6)$$

where $\#P(t, x)$ is the number of non-$\perp$ components of $P(t, x)$.

Proof: Each $\mathcal{S}_i = [0, T] \times \mathbb{R}$ and Φ has rank defect one (since the transmitters are not synchronized to a common source). Thus, at (x, t) the signal profile has depth $2\#P(x, t) - 1$, and for injectivity one needs,

$$2 \dim \mathcal{D} + 2 < \mathrm{dep}\, \mathcal{P} = 2\kappa - 1.$$

∎

D. Multi-modal sensing and fusion

Since genericity can be decoupled from each of the transmission functions independently, there is no reason why each should represent the same kind of signal modality. In contrast to some of the examples in the previous sections, we could well consider a heterogeneous family of transmitters. For instance, consider the situation where there are N transmitters for whom the receivers can detect signal strength only, but there are M for which signal strength and doppler can be measured. In this case, $\mathcal{S} = (\mathbb{R} \sqcup \perp)^N \times (\mathbb{R}^2 \sqcup \perp)^M$, which leads to $\mathrm{dep}\, \mathcal{P} = N + 2M$. A consequence of this situation is that one can imagine design constraints that balance the availability of inexpensive transmitters with more expensive (but more capable) transmitters. The reader may easily generalize.

E. Configuration spaces

There is no reason why $\mathcal{D}$ must conform to a physical or even physical-temporal locus of receivers. Consider the dual setting in which N receivers are fixed at locations in a physical domain X (a compact manifold with corners). A collection of M transmitters operate at distinct locations in X. The parameter space (to be embedded in a signals space) is the space of configurations of the M (labeled) transmitters, $\mathcal{C}^M(X) = X^M - \Delta_X$, where $\Delta_X = \{x_i = x_j \text{ for some } i \neq j\}$. Let $\mathcal{D} = \mathcal{C}^M(X)$, where, to ensure compactness, one removes a sufficiently small open neighborhood of the pairwise diagonal Δ_X. For simplicity, consider the restricted case where all N receivers can hear all M transmitters, and that the received signals are scalar-valued. The following result uses Theorem **??** to derive the existence of triangulation-without-distance algorithms: one can triangulate position based on a non-isotropic signal without knowledge of locations or actual distance.

Corollary 11. *Under the above assumptions, the transmitter positions are unambiguous for $N > 2 \dim X$, independent of M.*

Proof: From Theorem **??**, the criterion is:

$$2M \dim X = 2 \dim(\mathcal{C}^M(X)) < \dim \mathcal{S} = MN.$$

∎

In particular, for a planar domain, the positions of the transmitters is uniquely encoded in signal space by *five* fixed receivers, independent of the number of (audible) transmitters, providing a dual to Corollary **??**. Five exceeds the three needed for triangulation of position via geometry: for weaker topological signals, more data is required.

V. QUANTIZATION

Discretized signals would seem to promise effective localization. However, a straightforward application of Theorem **??** fails: using a quotient map Φ (recall §**??**) from $\mathcal{S}$ to a finite set (of dimension zero) yields a $\mathcal{P}$-weighted depth $\mathrm{dep}\, \mathcal{P} = 0$. Clearly, a quantized signal profile cannot be injective; however, if the quantization is fine enough, quantized signals should distinguish points in $\mathcal{D}$ up to some small distance.

The following result indicates that inversion of the signal profile is generically continuous, by showing that points which are close in $\mathcal{R}$ must have preimages that are close in $\mathcal{D}$. We begin by specifying a geometry on $\mathcal{S}$: suppose that each $\mathcal{S}_i$ is a Riemannian manifold, with induced metric d_i. The metric on $\mathcal{S}$ is the product metric on the d_i, with the (intrinsic) convention that d takes on the value ∞ if the points are in distinct connected components of $\mathcal{S}$.

Proposition 12. *Let $\mathcal{P} : \mathcal{D} \to \mathcal{R}$ be a received signal profile with stable domains $\mathcal{U} = \{U_i\}_1^N$ satisfying the assumptions of §**??**, with, in addition: (1) $\mathcal{S}$ and $\mathcal{R}$ are Riemannian on connected components; and (2) $\mathrm{dep}\, \mathcal{P} > 2 \dim \mathcal{D}$. For individual transmission signal maps $\mathcal{T}_i$ open and dense in $C^\infty(U_i, \mathcal{S}_i)$, and for $\epsilon > 0$ small, there exists a constant $K(\epsilon) > 0$ such that:*

$$\mathrm{diam}\, \mathcal{P}^{-1}\left(B_\epsilon(\mathcal{P}(x))\right) < K(\epsilon)$$

uniformly in $x \in \mathcal{D}$, with $\lim_{\epsilon \to 0^+} K(\epsilon) = 0$.

Proof: Recall from the proof of Theorem **??** the cover $\mathcal{V} = \{V_J\}$ of $\mathcal{D}$ by compact closures of the intersection lattice of the stable sets $\mathcal{U}$. From the hypothesis on $\mathrm{dep}\, \mathcal{P}$, the restriction of $\mathcal{P}$ to each V_J (with the canonical extension to any added boundary components) is a smooth embedding of V_J onto its image. Smoothness and compactness yields a function $K_J(\epsilon)$ bounding the diameters of preimages of the restriction. As $\mathcal{V}$ is finite, there is a uniform $K(\epsilon)$ for which the result holds. ∎

This result indicates that a quantization on the received signals space yields an ambiguity in the domain $\mathcal{D}$ of bounded size; this in itself is suboptimal, since the bounds might be poor.

VI. EXPERIMENTAL VALIDATION

To compensate for lack of hard bounds on quantization ambiguity, and to test the applicability of the Signals Embedding Theorem, we constructed two simple experiments. The first experiment is a computer simulation of acoustic

propagation, and the second uses acoustic hardware that we constructed. The platform-independence of Theorem **??** gives considerable freedom in selecting the transmitted waveforms and the construction of the experiments. Since we focus on the topological characterization of a propagation domain in this article, we conducted our experiments to demonstrate:

1) The correctness of our our axiomatic characterization of the signal profile;

2) That the resulting signal profile is injective (and remains so up to a reasonable signal-to-noise ratio), and furthermore;

3) That it is possible to detect a change in the homotopy type of the domain (roughly, the number of holes in the domain) by means of the signal profile measured at a collection of receiver locations.

The available tools for manipulating the resulting signal profile and its image are primitive. We have explicitly avoided the treatment of any methodology for inverting an injective signal profile. Clearly, when robust metric information is present (GPS, remote sensing, medical imaging, and many other contexts), inversion of signal profiles has been extremely important. However, very few algorithms (beyond the primitive ones shown here) are tailored to treat noisy signal profiles topologically.

A. Computer simulation

To provide a direct verification of the injectivity and continuity (when globally stable) of signal profiles, we conducted a numerical simulation of the propagation of acoustic waves in a topologically nontrivial 2-dimensional domain. We selected a domain with a single rectangular obstacle, as shown in Figure **??** (note that the region marked "Domain" corresponds to the measurement domain in the second experiment; the domain in the simulation was considerably larger). According to Corollary **??**, to exploit signal level or TOA requires 5 distinct transmitters, but to use TDOA (Corollary **??**) we require 6. In order to determine how tight these bounds are, we simulated a case with 4 transmitters. We computed the signal level and TOA for each of these transmitters, using a wavefront propagation code [**?**]. In order to simplify interpretation of the simulated results, we did not incorporate diffraction into the model.

The simulated signal levels for each transmitter are shown in Figure **??**. The simulated TOA plots look qualitatively similar to the signal level ones, but are reversed in color since the TOA is small near each transmitter. Resulting projections of the 4 dimensional signal space for signal level and TOA are shown in Figure **??**, where it should be noted that color is one of the dimensions. In both of these cases, it is visually apparent (though perhaps difficult to see from the plots exhibited here) that the signal profiles are injective. Additionally, since the stable regions U_i each individually cover the domain, the resulting profiles could theoretically be embeddings. That they actually are embeddings is clear from Figure **??**, due to the presence of the hole.

In contrast, there is an additional dimensional deficiency if a TDOA signal profile is used. This case is shown in Figure **??**,
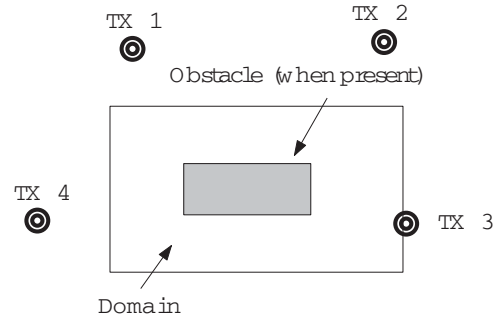

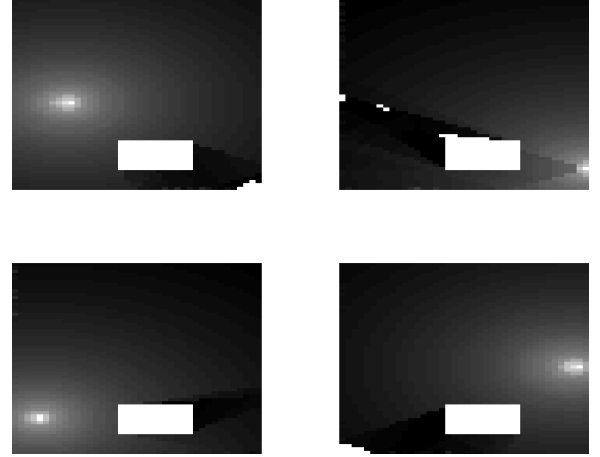Fig. 1.   Spatial layout of the experiment.

Fig. 2.   Received signal level for each of the four simulated transmitters. White indicates higher signal level, black indicates low signal level, measured in decibels.

where we note that color is not an independent dimension. In this case, there is a generic self-intersection in the image of the signal profile, which belies a lack of injectivity.

B. Hardware overview

Several transmitters were constructed (see Figure **??**) from a PIC16F88 microcontroller, a simple audio pre-amplifier, and a speaker. The microcontroller runs custom firmware that causes
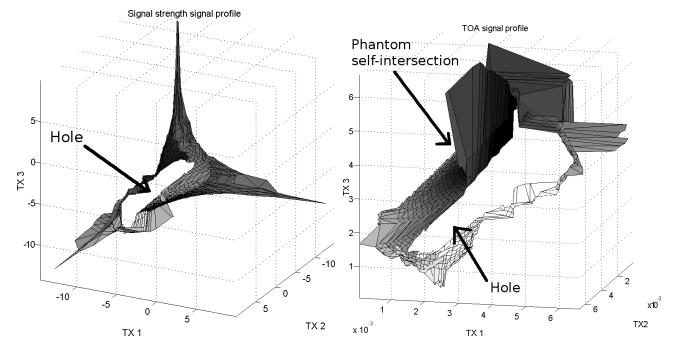

Fig. 3.   An illustrative projection of the signal level (left) and TOA (right) signal profiles in four dimensions for our simulation. The cardinal axes correspond to the signal level or TOA from TX 1-3, while the color corresponds to TX 4.
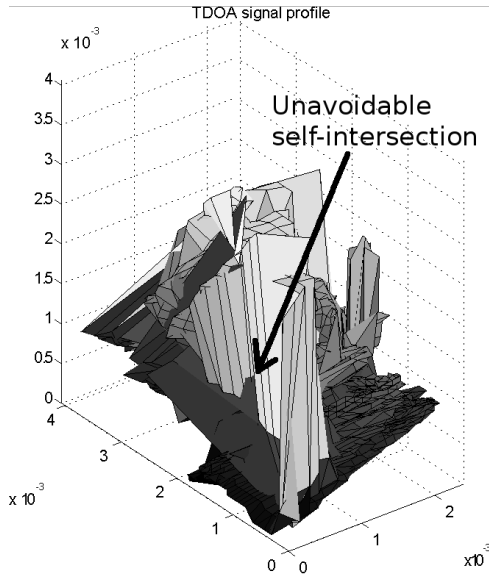
Fig. 4. An illustrative projection of the TDOA signal profiles in three dimensions for our simulation. The cardinal axes correspond to the subsequent time differences as discussed in §**??**. Note that color corresponds to the vertical direction, unlike Figure **??**.
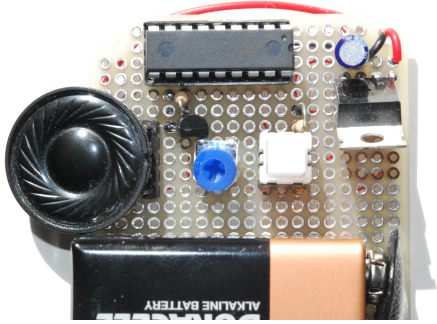

Fig. 5. Acoustic sounders that were constructed to be transmitters in experiments.

the sounder to emit square waves with arbitrary transition times in the range of 5kHz-10kHz. Signal reception was accomplished by the use of a standard laptop computer sound card. The computer ran a custom real-time matched filter bank (using the GStreamer multimedia framework) tuned to each of the transmitters. When triggered by the user, the computer stored the magnitude of each matched filter tap in a data file for later processing.

We endeavored to conduct a physical experiment that mirrored our simulation results. Since both signal level and TOA signal profiles appeared to be embeddings but TDOA does not, we selected the same configuration of transmitters and domain as used in our simulation.

The experiment was conducted on a laboratory floor cleared of acoustically reflective obstacles in the immediate vicinity. Scatterers were present outside of the experimental area, resulting in potential multipath returns. For each run of the experiment, transmitters were placed at the fixed locations (labeled 1-4 as in the simulation), and the receiver was raster-

TABLE I
LISTING OF EXPERIMENTAL RUNS.

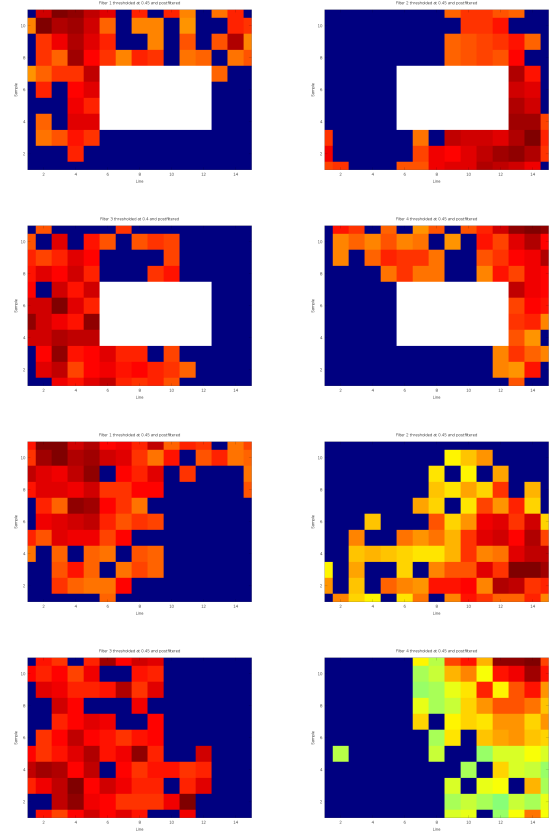| Run	Obstacle	Transmitters	Comments
A	No	1, 2	Calibration run (not shown)
B	Yes	1, 3	Experimental collection
C	Yes	2, 4	Experimental collection
D	No	1, 3	Experimental collection
E	No	2, 4	Experimental collection

Fig. 6. Thresholded signal levels from each transmitter as a function of position. The top four frames represent runs B,C. Missing portions of the data correspond to the presence of the obstacle.

scanned throughout the experimental domain (avoiding any obstacles) with a spacing of 3 inches between samples. For two of the runs, an acoustically opaque obstacle (a stack of books) was placed within the experimental volume. See Figure **??** for details of the layout and Table I for a listing of the experimental runs. Runs B and C collectively consider the case where there is an obstacle in the domain (and so the domain is an annulus), while D and E address the case when the domain is contractible.

C. Validation of signal model

The received signal levels corresponding to each transmitter are displayed in Figure **??**, which incorporates a choice of signal level threshold (independently for each transmitter) to simulate the failure of reception. These plots also incorporate some spatial filtering (averaging of the signal levels from adjacent sample points) to compensate for receiver instability.
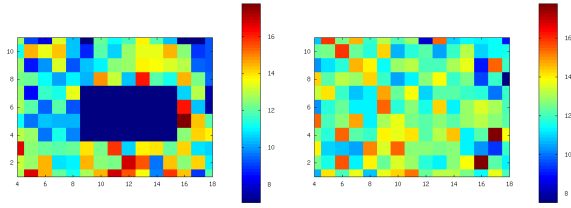
Fig. 7. Signal-to-noise ratio required to maintain injectivity of the signal profile at a given receiver location in runs B,C (left) and runs D,E (right)
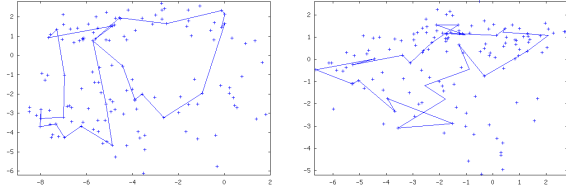

Fig. 8. Projection of received signal levels at each receiver. The data from runs D,E (right) have been randomly downsampled to match the number of points in runs B,C (left). The marked path tightly bounds the obstacle, when it is present.
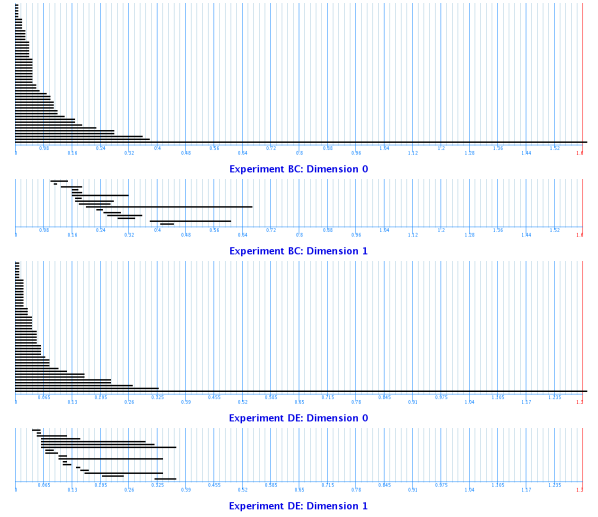

Fig. 9. Persistent homology barcodes of the two collection runs. The top two correspond to the experiments with an obstacle (B and C), and the bottom two correspond to the experiments without an obstacle (D and E).

This latter processing improves the smoothness of the plots but does not materially change the results. It is immediately clear from these plots that there is a stable domain containing each transmitter, and that away from this domain the reception becomes erratic before dropping out completely. We regard this as a validation of assumption (2) of the signal profile.

Given the experimentally collected data, it is straightforward to infer properties of the signal profile. In this experiment, the quantized signal profile was injective, in that each receiver location had a unique response to the set of transmitters. Given the potentially large dynamic range of the data, we found that 18 dB of signal-to-noise ratio was required to ensure that the resulting quantized signal profile remains injective. Figure **??** shows the lowest signal-to-noise ratio required to maintain injectivity at a given receiver location, and indicates that this is fairly stable over the domain with an average value of roughly 15 dB for both sets of runs. (We computed Figure **??** by finding the radius of the largest ball around each measurement whose preimage was connected.) It should be noted that in this sense, signal-to-noise ratio is a *metric* property of the signal profile. Although a signal profile may be an embedding in a topological sense, if the resulting profile under a perturbation is not an embedding, it may be difficult to exploit our theory. Our experiments have therefore demonstrated that this unhappy situation does not occur even with relatively simple equipment.

D. Topological characterization of the domain

The maximal depth of the cover in this experiment is *three*, which is below the required (*five*) for guaranteed signal profile injectivity. However, even this appears to suffice for the purposes of detecting the difference in topological type of the domains used in runs B,C versus D,E. To see this, first consider the projection of the data into two dimensions given

in Figure **??**. Using the formulae in [**?**] with the appropriate values from the experiment results in a likelihood of about 10% that a random projection will be sufficiently close to an isometry to be topologically accurate. Instead, we have plotted a particularly illuminating projection, in which the cardinal axes are the differences in signal levels between TX 1 and 3 (horizontal), and between TX 2 and 4 (vertical). The plot on the left clearly shows a "hole" (in the interior of the path) that gives the location of the obstacle. The plot on the right shows no such hole, and indicates that no obstacle is present.

Evidently the projection in Figure **??** is far from random, so it is desirable to have a more objective measure of the validity of detection of the topological. Recently, PERSISTENT HOMOLOGY has emerged as an effective tool for examining the topology of point clouds sampled from a topological space [**?**], [**?**]. This algebraic method discriminates between a contractible planar domain and one punctured by obstacles. In particular, the presence of a persistent generator of homology in dimension one (H_1) indicates the presence of an obstacle. We computed this persistent homology using JPlex [**?**]; its signature, or BARCODE, is shown in Figure **??**. Briefly, persistent homology counts path components and holes present in a family of spaces related to a discrete subspace of a metric space. Rather than considering the discrete space (our measurements) directly, one considers a union of balls of a varying (common) radius centered on each point. The horizontal axis in Figure **??** corresponds to the radius of these balls: smaller is on the left and larger is on the right. In our data, these radii are inversely proportional to signal-to-noise ratio and the horizontal units in Figure **??** are in decibels. Each horizontal bar corresponds to a connected component (in dimension 0) or a nontrivial loop (in dimension 1). Longer bars correspond to features that "persist" for more choices of radius, and therefore are considered more important. Conversely, shorter bars are considered to be the effect of noise.

It is immediately clear that both runs came from connected

domains (since there is one dimension 0 bar that persists for almost all scales). There are some persistent generators in dimension 1 (holes) for both sets of runs, but there is only one substantial hole in experiments B and C that persists in excess of 0.5 dB. This indicates the strong possibility of the presence of a 1-dimensional hole in the domain for the case of runs B and C but not in runs D and E. Hence, we conclude that the experiment has detected a topological change in the domain, and in particular identifies the presence of one obstacle in runs B and C and no obstacles in D and E.

VII. CONCLUSION

This paper builds a general theoretical framework in which to analyze signals of opportunity and utilize such to characterize a domain in terms of a representation into the appropriate space of signals.

Our approach could be exploited to permit localization in contexts where it is presently impossible, and may provide a mechanism to exploit GPS or other reference signals that are heavily corrupted due to uncertainty about multipath, transmitter position, timing, and power level.

Of note in our approach are the following features:

1) Instead of trying to reconstruct coordinates within the domain, it can be effective and profitable to work completely within the space of signals. Given sufficient control over the signal profile depth, this representation is faithful, modulo the discontinuities induced by limited-extent signals.

2) One advantage of working within a space of signals is the independence of the signal type. The topological approach reveals that dimension is the critical resource for faithful representation.

3) Although the differential-topological tools used assume a high degree of regularity and ignore noise and other inescapable system features, the robustness of the results to quantization — as verified in theory, simulation, and experiment — argues for wide applicability.

ACKNOWLEDGMENT

REFERENCES

[1] R. D. *et al.*, "World-wide lightning localization using VLF propagation in the earth-ionosphere waveguide," *Antennas and Propagation Magazine*, vol. 50, no. 5, pp. 40–60, October 2008.

[2] H. Lee and H. Aghajan, "Collaborative node localization in surveillance networks using opportunistic target observations," in *VSSN '06*, October 2006.

[3] Y. Baryshnikov and J. Tan, "Localization for anchoritic sensor networks," *Proc. DCOSS*, pp. 82–95, 2007.

[4] E. Hanle, "Survey of bistatic and multistatic radar," *IEE Proc.*, vol. 133 Pt. F, no. 7, December 1986.

[5] J. M. Hawkins, "An opportunistic bistatic radar," in *Radar 97*, 1997, pp. 318–322.

[6] B. R. Breed and W. L. Mahood, "Multi-static opportune-source-exploiting passive sonar processing," US Patent Application, Tech. Rep. 2003/0223311 A1, 2003.

[7] L. Carin, H. Liu, T. Yoder, L. Couchman, B. Houston, and J. Bucaro, "Wideband time-reversal imaging of an elastic target in an acoustic waveguide," *J. Acoust. Soc. Am.*, vol. 115, no. 1, pp. 259–268, January 2004.

[8] R. Zetik, J. Sachs, and R. Thomä, "Imaging of propagation environment by UWB channel sounding," EURO-COST, Tech. Rep. COST 273 TD(05)058, 2005.

[9] P. Viswanath, D. N. C. Tse, and R. Laroia, "Opportunistic beamforming using dumb antennas," *IEEE Trans. Info. Theory*, vol. 48, no. 6, pp. 1277–1294, 2002.

[10] S. VanLaningham, J. A. Stevens, A. K. Johnson, and R. A. Rivera, "System and method for target location," Rockwell Collins, Tech. Rep. U.S. Patent 7782247, 2010.

[11] B. Yazıcı, M. Cheney, and C. E. Yarman, "Synthetic-aperture inversion in the presence of noise and clutter," *Inverse Problems*, vol. 22, pp. 1705–1729, 2006.

[12] M. Cheney and B. Yazıcı, "Radar imaging with independently moving transmitters and receivers," in *Defense Advanced Signal Processing*, 2006.

[13] G. J. F. M. A. Ringer and S. J. Anderson, "Waveform analysis of transmitters of opportunity for passive radar," Australian Defense Science and Technology Organization, Tech. Rep. DSTO-TR-0809, 1999.

[14] R. Saini and M. Cherniakov, "Dtv signal ambiguity function analysis for radar application," *IEE Proc.-Radar Sonar Navig.*, vol. 152, no. 3, pp. 133–142, June 2005.

[15] H. J. Yardley, "Bistatic radar based on DAB illuminators: The evolution of a practical system," in *IEEE Radar Conf.*, 2007.

[16] C. Coleman and H. J. Yardley, "Passive bistatic radar based on target illuminations by digital audio broadcasting," *IET Radar Sonar Navig.*, vol. 2, no. 5, pp. 366–375, 2008.

[17] M. Radmard, M. Bastani, F. Behnia, and M. M. Nayebi, "Advantages of the dvb-t signal for passive radar applications," in *IEEE Radar Symposium*, 2010.

[18] K. Browne, R. Burkholder, and J. Volakis, "High resolution radar imaging utilizing a portable opportunistic sensing platform," in *Antennas and Propagation Society International Symposium (APSURSI), 2010 IEEE*, July 2010, pp. 1 –4.

[19] J. G. O. Moss, A. M. Street, and D. J. Edwards, "Wideband radio imaging technique for multipath environments," *Electronics Letters*, vol. 33, no. 11, pp. 941–942, 1997.

[20] M. Cheney and R. J. Bonneau, "Imaging that exploits multipath scattering from point scatterers," *Inverse Problems*, vol. 20, pp. 1691–1711, 2004.

[21] C. J. Nolan, M. Cheney, T. Dowling, and R. Gaburro, "Enhanced angular resolution from multiply scattered waves," *Inverse Problems*, vol. 22, pp. 1817–1834, 2006.

[22] J. W. Melody, "Predicted-wavefront backprojection for knowledge-aided sar image reconstruction," in *IEEE Radar Conf.*, 2009.

[23] V. Krishnan, C. E. Yarman, and B. Yazıcı, "Sar imaging exploiting multipath," in *IEEE Radar Conf.*, 2010, pp. 1423–1427.

[24] D. R. Hundley and M. J. Kirby, "Estimation of topological dimension," in *Proc. Third SIAM Conf. Data Mining*, vol. 3, 2003, pp. 194–202.

[25] F. Camastra, "Data dimensionality estimation methods: A survey," *Pattern Recognition*, vol. 36, no. 12, pp. 2945–2954, 2003.

[26] M. B. Wakin, "The geometry of low-dimensional signal models," Ph.D. dissertation, Rice University, 2006.

[27] M. B. Wakin and R. G. Baraniuk, "Random projections of signal manifolds," in *ICASSP*, 2006, pp. 941–944.

[28] K. L. Clarkson, "Tighter bounds for random projections of manifolds," in *Proceedings SoCG*, New York, NY, 2008, pp. 39–48.

[29] J. B. Tenenbaum, V. de Silva, J. C. Langford, "A Global Geometric Framework for Nonlinear Dimensionality Reduction," *Science* 290, pp. 2319-2323, 2000.

[30] A. Singer and H.-T. Wu, "Orientability and Diffusion Maps", *Applied and Computational Harmonic Analysis*, 31 (1), pp. 44–58, 2011.

[31] R. Coifman and S. Lafon, "Diffusion Maps." *Science*, 19 June 2006.

[32] D. Donoho and C. Grimes, "Hessian eigenmaps: Locally linear embedding techniques for high-dimensional data." *Proc Natl Acad Sci* 100(10): 5591-5596, May 13, 2003.

[33] G. Peyré, "Image processing with non-local spectral bases," *SIAM J. Multiscale Modeling and Simulation*, vol. 7, no. 2, pp. 703–730, 2008.

[34] M. B. Wakin, "A manifold lifting algorithm for multi-view compressive imaging," in *Picture Coding Symposium*, 2009.

[35] ——, "Manifold-based signal recovery and parameter estimation from compressive measurements, `arxiv:1002.1247v1`," 2010.

[36] J. Nash, "The imbedding problem for riemannian manifolds," *Ann. of Math., Second Series*, vol. 63, no. 1, pp. 20–63, January 1956.

[37] R. G. Baraniuk, "Manifold-based image understanding," Rice University, Tech. Rep., 2007.

[38] A. Vasy, "Propagation of singularities for the wave equation on manifolds with corners." *Ann. of Math*, vol. 168, pp. 749–812, 2008.

[39] G. Carlsson, "Topology and Data," *Bulletin of the American Mathematical Society*, vol. 46, no. 2, pp. 255–308, January 2009.

[40] A. Zomorodian and G. Carlsson, "Computing persistent homology," *Discrete and Computational Geometry*, vol. 33, no. 2, pp. 247–274, January 2005.

[41] M. Robinson, "Inverse problems in geometric graphs using internal measurements, arxiv:1008.2933," 2010.

[42] M. Robinson, "A wavefront launching model for predicting channel impulse response," *ACES Journal*, vol. 22, no. 2, pp 302–305, July 2007.

[43] M. Hirsch, *Differential Topology*. Springer-Verlag, 1976.

[44] M. Golubitsky and V. Guillemin, *Stable Mappings and Their Singularities*. Springer-Verlag, 1973.

[45] J. Margalef-Roig and E. O. Dominguez, *Differential Topology*. Amsterdam: North-Holland, 1992.

[46] H. Sexton and M. Vejdemo-Johansson, "JPlex simplicial complex library. http://comptop.stanford.edu/programs/jplex/," 2011.

Michael Robinson is a postdoctoral fellow in the Department of Mathematics at the University of Pennsylvania. His 2008 Ph.D. in Applied Mathematics [Cornell University] and recent work in topological signal processing is complemented by a background in Electrical Engineering and current work in radar systems with SRC, Syracuse, NY.

Robert Ghrist is the Andrea Mitchell University Professor of Mathematics and Electrical & Systems Engineering at the University of Pennsylvania. Ghrist is a (2004) PECASE-winning mathematician and a Scientific American SciAm50 winner (2007) for leadership in research. His specialization is in topological methods for applied mathematics.

APPENDIX

A DIFFERENTIAL n-MANIFOLD is a paracompact Hausdorff space M with an open covering $\mathscr{U} = \{U_\alpha\}$ and maps $\phi_\alpha : U_\alpha \to \mathbb{R}^n$ which are homeomorphisms onto their images and for which the restriction of $\phi_\beta \phi_\alpha^{-1}$ to $U_\alpha \cap U_\beta$ is a smooth (C^∞ for our purposes) diffeomorphism whenever $U_\alpha \cap U_\beta \neq \emptyset$. One says that an n-manifold is MODELED on $\mathbb{R}^n$ via CHARTS U_α in an ATLAS $\mathscr{U}$. An n-manifold with BOUNDARY is a space locally modeled on $\mathbb{R}^n$ or the upper halfspace $\mathbb{R}^+ \times \mathbb{R}^{n-1}$, depending on the chart. An n-manifold with CORNERS allows a choice of any $(\mathbb{R}^+)^k \times \mathbb{R}^{n-k}$ as local models.

To each point p in a manifold M is associated a TANGENT SPACE, $T_p M$, a $\mathbb{R}$-vector space of dimension $\dim M$ that records tangent data at p. The collection of tangent spaces fit together into a TANGENT BUNDLE, a manifold $T_* M$, defined locally as charts of M crossed with $\mathbb{R}^{\dim M}$. Maps between manifolds are said to be smooth if the restriction of the map to charts yields smooth maps between charts. Such maps $f : M \to N$ induce a DERIVATIVE $Df : T_* M \to T_* N$ defined on charts via the Jacobian derivative. The JET BUNDLE $J^r(M, N)$ is the manifold which records all degree r Taylor polynomials associated to maps in $C^r(M, N)$, with the topology inherited from M (source points), N (target points), and the usual topology on real coefficients of polynomials. We use C^∞ smoothness in this paper, and place the usual (Whitney) C^∞ topology on the space $C^\infty(M, N)$ of smooth maps from M to N: a C^∞ neighborhood of $f : M \to N$ has basis functions g whose r-jets are close, as measured by the topology on $J^r(M, N)$.

A subset $A \subset X$ is RESIDUAL if it is the countable intersection of open dense subsets of X. For BAIRE spaces, like $C^\infty(M, N)$, residual sets are always dense. A property is GENERIC (or holds generically) with respect to a parameter space if that property is true on a residual subset of the parameter space.

Two submanifolds V, W in M are transverse, written $V \pitchfork W$, if and only if $T_p V \oplus T_p W = T_p M$ for all $p \in V \cap W$ — the tangent spaces to V and W span that of M at intersections. Note that the absence of intersection is automatically transverse. A smooth map $f : V \to M$ to a submanifold $W \subset N$ if and only if $Df_v(T_v V) \oplus (T_p W) = T_p M$ whenever $f(v) = p$. The JET TRANSVERSALITY THEOREM states that for W a submanifold of $J^r(M, N)$, the set of maps in $C^\infty(M, N)$ whose r-jets are transverse to W is residual. This readily yields the simpler transversality theorem that the subset of $C^\infty(M, N)$ transverse to a submanifold $W \subset N$ is residual (and, furthermore, open if W is closed).